Journal of Applied Fluid Mechanics, Vol. 8, No. 4, pp. 667-672, 2015.
Available online at www.jafmonline.net, ISSN 1735-3572, EISSN 1735-3645.
DOI: 10.18869/acadpub.jafm.73.238.20428

A Study of the Complex Flow Features Behind a Diffracted Shock Wave on a Convex Curved Wall

A.O. Muritala[1†], B.W. Skews[2] and L. Craig[2]

[1] *Obafemi Awolowo University, Ile-Ife, Osun State, 220005, Nigeria*
[2] *School of Mechanical, Industrial and Aeronautical Engineering, University of The Witwatersrand, PO WITS 2050, South Africa*

†*Corresponding Author Email: muriadam@oauife.edu.ng*

(Received June 12, 2013; accepted November 10, 2014)

ABSTRACT

The complex flow features behind a diffracted shock wave on a convex curved wall is investigated using large scale experimentation complemented by numerical computation. The study aimed at explaining the global flow behavior within the perturbed region behind the diffracted shock wave. Experiments were conducted in a purpose built shock tube that is capable of generating a range of incident shock Mach numbers Mn ≤ 1.6. Analysis of higher Mach number shocks on different wall geometries were carried out using numerical code that has been validated by earlier authors. Many flow features that were only distinct at high Mach numbers are clearly identified at low Mach numbers in the present investigation. The separation point moves upstream at incident shock Mach number Mn = 1.5 but moves downstream at higher Mach numbers and is nearly stationary at Mn = 1.6. At incident shock Mach number 3.0 the movement of the separation point tends to be independent of the wall curvature as the wall radius approaches infinity. The present investigation is important in the design of high speed flow devices and in the estimation of flow resistance on supersonic devices and space vehicles.

Keywords: Compressible flow; Shock wave diffraction; Shear layer; Flow separation.

NOMENCLATURE

Mn	Mach number	CFL	Courant number in Fluent
r	cylinder radius	k	calibration constant of the transducer
α	parameter to define incident shock position	V_i	voltage recorded at position i
P_i	static pressure at point i	dt	time step

1. INTRODUCTION

Engineering applications such as design of exhaust manifold of an internal combustion engine; profile selection for missiles and design of supersonic vehicles and devices require detailed understanding of the flow behavior behind a moving shock wave.

This is because high speed compressible flows are characterized by shock waves which are mechanical waves of finite amplitude propagated by coalescence of several disturbance waves over a very short period of time.

A common phenomenon that is encountered by a shock wave is diffraction process. This occurs when a shock wave traverse over a convex curved wall. The shape, strength and the orientation of the planar shock change with time as a result of the disturbances propagated by a change in wall geometry (Ben-Dor et al., 2001).

The diffraction of a normal shock wave motivates the compression of the gas particles adjacent to the shock. This compression process is unsteady with region of flow perturbation behind the diffracted shock. Within this region the flow separates from the wall surface due to the presence of adverse pressure gradient. Shear layer evolved from the separating region with other flow features that can only be captured by carefully arranged optical devices.

Understanding of the complex flow features behind a diffracted shock wave plays a very important role in the design of supersonic flow devices such as

blast wave attenuator against terror attacks, exhaust nozzles of an internal combustion engine, gas transmission line, supersonic jet engines, selection of optimum profile for missiles, etc.

Earlier works by Skews (1967a&b) have observed some flow features in a series of experiments that were conducted in a conventionally sized shock tube. Around the perturbed region behind the diffracted shock wave a shear layer, an oblique shock and a second shock were observed. A centered - expansion fan was observed at the corner and the diffraction process is self-similar.

Further work by Law et al. (2005) on shock wave diffraction has both temporal and spatial scale limitations. The flow behavior behind the diffracting shock could not be examined at long times due to undesirable interaction with the reflection of the incident diffracted shock from the bottom wall of the test section.

Another study by Skews (2005) involves experimental analysis with conventionally sized shock tube combined with analytical approach using Whitham's theory. A good prediction of the shape and the orientation of the diffracting shock wave on curved walls were obtained. The result of the analysis revealed that there is no separation at incident shock of Mach number 1.5 on 68mm diameter wall for the maximum obtainable diffraction time.

The boundary layer along the wall became thick especially at higher value of Mα/r (M Mach number, r radius and [α], a parameter to define incident shock displacement). Mα/r is the parameter that determines the position of the diffracting shock. The results also suggested possible separation of the flow if Mα/r is significantly high. However, the small scale shock tube used for the experiments could not accommodate higher values of this influencing parameter.

Muritala et al. (2010) has explained the transient development of weak shock waves within the perturbed region behind the diffracted shock wave on curved walls using numerical computation. A three shock configuration was observed at low incident shock Mach numbers while multiple shock configurations were reported for high Mach number incident shocks. The study could not explained the turbulent flow behaviour due to limited experimental facility.

Muritala et al. (2011) used a large scale experiment to explain the behavior of the separation point on a curved wall. The analysis captured the separation phenomenon at low incident shock Mach numbers. Further work by Muritala et al. (2013) presented the pressure history of a diffracting shock wave on 200mm diameter wall. The fluctuations in pressure traces were used to locate region of instability along the wall surface. It was observed that the rate at which the flow instability is propagated along upstream is different from downstream.

Skews et al. (2012) has conducted a large scale experiment in a specially built shock tube to explain the shear layer resulting from a diffracted shock wave on angular geometries. It was discovered that there is a breakup of the shear layer into vortices at an incident shock Mach number 1.5 over a ninety degree corner wall. This explains the earlier numerical results obtained by Sun and Takayama (2003) which could not be explained by the results of experiments conducted in a conventional shock tube.

The present investigation examines the complex flow structure behind the diffracted shock wave using both experimental and numerical technique to explain the global flow behaviour behind the diffracted shock wave.

2. EXPERIMENTAL PROCEDURE

Experiments were conducted in a purpose built shock tube that is made up of a 2m long circular driver section of diameter 0.45m, joined to three 2m long rectangular driven section with a cross – sectional area of 0.1m x 0.45m.

The driver and the driven sections are separated by a diaphragm which is made of plastic sheet. The driver section of the shock tube is operated with a control panel with valves and a pressure gauge.

The test gas is air and is considered thermally and calorically perfect because the tests were carried out over a range of incident shock Mach numbers Mn ≤ 1.6. The ambient temperature and pressure were recorded at intervals during the experiments.

The test section has internal cross - sectional area of 1.105m x 0.1m with a length of 2m. There are two circular glass windows of diameter 0.30m enclosed in a circular frame of diameter 1m. One of the glass windows is divided into square grids by tiny string for estimation of the size of a flow feature of interest. The circular domain that housed the test windows is designed such that it can rotate through an angle of 360° to facilitate proper alignment of the surface of interest as shown in Figure 1.

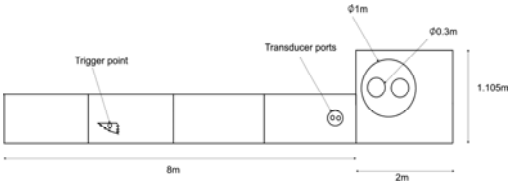

Fig. 1. Diagramatic representation of the experimental shock tube.

The model is fixed in the test section within the glass window such that the surface of interest is located within the field of view of the optical system. There are two transducer ports on the driven section located close to the inlet of the test section; these ports housed the transducers that measure the pressure rise across the incident planar shock wave. The distance between the two transducers is 0.05m and the first port is about

0.49m from the start of the diffracting surface. The transit time between the two transducers is used to calculate the velocity of the incident shock before the start of diffraction of the shock wave on the model.

The instrumentation consists of a time delay box, a 4 – channel Yogokawa oscilloscope (Model DL1540) that displays the pressure trace, 6 signal amplifiers (PCB Piezotronic 482 series) and 6 pressure transducers. The transducers were connected to the signal amplifiers and to the oscilloscope which displays the pressure trace at each port. A sudden rise in pressure indicates the instant of shock traversing the surface of the transducers. The shock velocity is determined from the distance between the two ports and the time taken by the shock to cover the distance between the transducers.

The approximate time taken by the shock to arrive at a particular location on the model is estimated based on the shock speed earlier determined from the two transducers on the driven section. This is used to set the time delay to trigger the light source which is employed to capture the interaction of interest at different position of the diffracting shock wave. The remaining four transducers were used to record the pressure traces on the surface of the model and were connected to the data logger through signal amplifiers. The locations of the transducers are designated by P_1, P_2, P_3, and P_4, and are located 50°, 60°, 70° and 80° from the inlet as shown in Figure 2.

The flow interaction behind the diffracting shock wave was captured using the schlieren visualization technique. The Z-Type 2-Mirror schlieren arrangement which is principally based on optical inhomogeneity of the flow field is used.

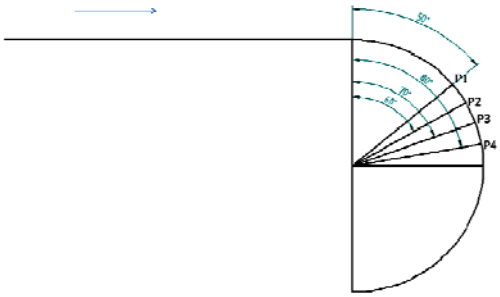

Fig. 2. Position of pressure transducers.

The pressure traces were recorded by the oscilloscope and displayed by a hard disc data logger GL1000 Graphtec using hard disc data logger software version 1.0. The trigger was set at the first channel which corresponds to port P_1.

3. NUMERICAL METHOD

Numerical computations were carried out using a commercial code (Ansys® Fluent) based on Reynolds Averaged Navier-Stokes equations (RANS). The flow is governed by the fundamental fluid dynamic principles; mass conservation, conservation of momentum and conservation of energy.

The density and pressure are related by the perfect gas law; this is justified by the fact that the maximum temperature is well below 1000K for the incident shock Mach numbers tested. The gas is assumed to be perfect and this necessitates the use of ideal gas equation to relate density and pressure.

The two turbulence models k-ε and k-ω were blended together by Menter (1993) to form SST k-ω turbulence model. The free stream independence of the k–ε turbulence model and the accurate prediction of the viscous effects of the flow close to the wall by k–ω turbulence model make the SST k–ω turbulence model more suitable for the present analysis. A damped cross-diffusion derivative term is used in the ω equation, and the turbulent viscosity is modified to cater for the transport of the turbulent shear stress. This model looks promising than both the k–ω and k–ε turbulence models especially in the analysis of a separating flow that requires adequate resolution of near wall effect without introducing unnecessary viscous dissipation outside the boundary layer. It has been confirmed accurate and more reliable for adverse pressure gradient flows Law et al. (2014).

The Reynold stresses in the equation are related to the mean velocity using the Boussinesq hypothesis. This hypothesis is used in Fluent in the k – ω and k – ε turbulence models because there is relatively low computational cost associated with the computation of turbulent viscosity. The Boussinesq hypothesis has two additional transport equations: for the turbulent kinetic energy k and either the turbulent dissipation rate ε or the specific dissipation rate ω. The turbulent viscosity is then computed in terms of k and ε.

The flow domain has three boundaries (inlet, outlet and no-slip) and was defined by a characteristic length which is the radius of the curved wall. This length was used to compute the dimensionless time which is defined by equation (1).

The dimensionless time scale is given by τ:

$$\tau = \frac{at}{c} \tag{1}$$

where c is the characteristic length (radius of the arc for the curved wall), t is the time from when the shock first arrives at the start of the curved wall and starts diffraction process, a is the sound speed in the undisturbed region ahead of the incident shock wave.

The dimensionless time describes how long the shock wave can diffract on the curved surface before it interacts with the reflected shock of the original incident shock wave. This is the parameter that determines the size of the experiment. It also makes the present result to be comparable with the earlier work by Skews (2005).

The inlet and outlet boundary were two characteristic lengths upstream and eight

characteristic lengths downstream of curved wall respectively. These lengths were chosen so that there is enough distance from the inlet to be sure that any numerical noise generated by the impulsive starting of the flow will be damped out. It will also ensure non-interference of the interaction of the incident shock with region of interest for the duration of the testing times considered.

The computational domain was discretized using unstructured quadrilateral cells with an initial cell size of 3 mm as shown in figure 3. The y^+ value was set to 11.63 in the region under the shear layer so that the boundary layer could be properly resolved. This lies within the recommended value of $5 \leq y^+ \leq 100$ specified for k-ω turbulence model implemented in Fluent. This is particularly important as the global flow features of interest are influenced by this.

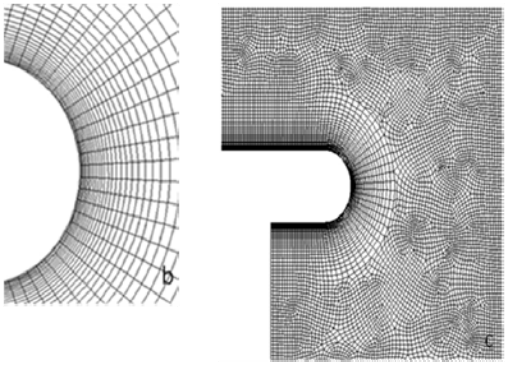

Figure. **3**. **The flow domain for the numerical computation**.

4. RESULTS AND DISCUSSION

Figure 4 is a graphical representation of the position of separation point (i.e angle between the separation point and the vertical line from the centre of the curved wall) for incident shock Mach number 2.0 on a 200mm diameter wall against number of meshes.

This is used to ascertain the independence of solution from the number of meshes. Since the solution adaptive mesh generation technique is used to fix the maximum number of meshes. The system generated more meshes at the region where there is a significant change in the flow parameters.

The solution approaches the asymptotic value of about 62.4 as the number of meshes tends to infinity. The solution became independent of the number of meshes as the number of meshes reached about 1,000,000 elements which is the minimum number of meshes considered for this work.

Figure 5 compared the numerical and experimental results obtained for an incident shock of Mach Number 1.6 diffracting on a 200mm diameter wall as earlier shown by Muritala (2011) and Law et al. (2014). The shear layer and the second shock which are some of the near wall flow features in the diffraction process are distinct in both pictures

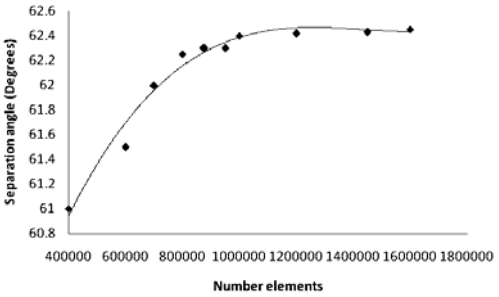

Fig. **4**. **Change in angle of separation as the number of elements increases.**

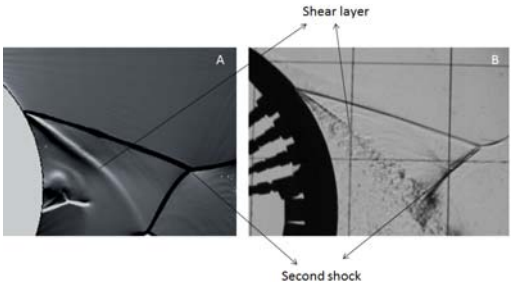

Fig. 5. Comparison of numerical and experimental results: A – Numerical and B – Experiment.

The diffraction process started immediately the incident shock (Mn 1.6) encountered the curved wall as shown in Figure 6. It bent backward and compressed the gas particles along the wall curvature resulting in perturbation. The flow development within the perturbed region started with an increase in boundary layer thickness as earlier observed by Muritala (2010). The thickness of the boundary layer extended downstream as the diffraction process continued. An adverse pressure gradient along the wall developed. Weak shock waves were propagated behind the diffracting shock and these shocks impinged on the boundary layer as the diffraction process progressed downstream.

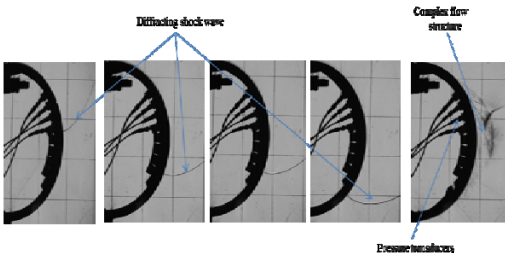

Fig. 6. Diffraction of a planar shock wave over a convex curved wall.

The thickness of the subsonic flow region within the boundary layer increases and the velocity of the flow decreases in order to satisfy no-slip condition at the wall. The shock wave/boundary layer interaction shows that when the incident shock impinges on the boundary layer the Mach number decreases as it approaches the wall. Information about the pressure rise within the subsonic region caused by the shock is sent upstream. This pressure increase upstream of the point of shock impinges the boundary layer causes the boundary layer to thicken as earlier observed by Craig et al. (2005).

Separation occurs when the pressure gradient is strong enough to overcome the viscous force along the wall surface. A shear layer evolves from the separation point and extends downstream as the diffraction progresses as shown in Figure 7. The lambda shocklets that formed above the shear layer coalesced into a second shock that brings the high speed flow upstream parallel to the flow along the shear layer as earlier observed by Muritala et al. (2011).

The movement of the separation point on a 200mm diameter wall for various Mach numbers is shown in Figure 8. The separation point moved upstream at an incident shock Mach number of 1.5 and is nearly stationary at 1.6. At higher incident Mach numbers the separation point moved in the downstream direction and varied significantly with time.

The anomaly movement of separation point between 1.5 and 1.6 incident shock Mach number may be attributed to the three dimensional nature of the experiments which has been captured in two dimensions. The flow features at low Mach number are mostly near wall flow features that require larger scale experimental facilities that can give longer time history of the flow behavior.

This observation revealed why the flow behavior at low Mach number is more complex than at high Mach number. The flow features at high Mach number are distinct even with small scale experimental analysis as earlier studied by Skews (2005).

The study also shows that between the incident shock Mach numbers 1.5 and 1.6, there is a threshold Mach number beyond which the separation point changes direction. The flow physics for this phenomenon needs further investigation as the present experiment is limited by spatial and temporal scales.

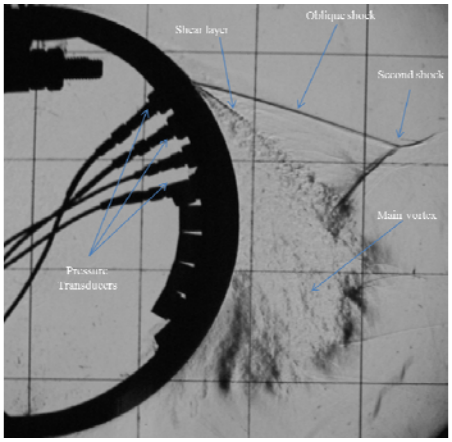

Fig. 7. The flow features at Mn = 1.6 on 200mm diameter wall at a time scale of about 1.1

The graph of the movement of the separation point along the wall curvature at incident shock Mach number 3.0 is shown for different wall geometries in Figure 9.

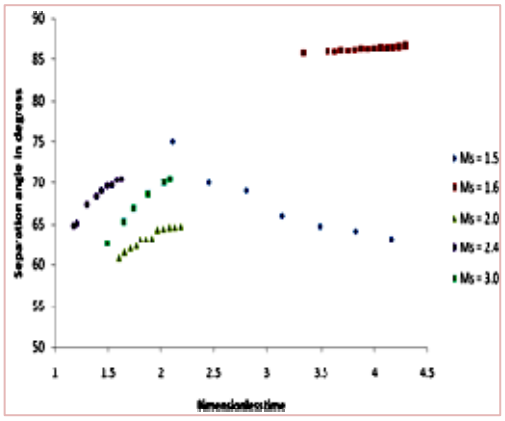

Fig. 8. Movement of separation point along the wall at different incident shock Mach number.

The separation angle increases with time for all wall geometry, however, the separation angle tends to be independent of wall curvature as the radius of the wall approaches infinity. The movement of the separation point will follow the same trend at incident shock Mach number 3.0 on wall profiles with diameters greater than 300mm.

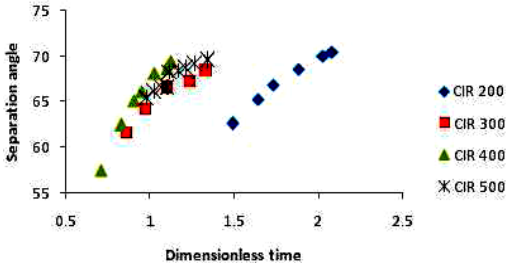

Fig. 9. Behavior of separation angle at Ms 3.0 on walls of different diameter.

The turbulent flow after the separation point shows there is higher pressure due to compressive effect of the diffracting shock. The turbulent patches are bounded above by the shear layer which is a line of velocity and temperature discontinuity. The flow under the shear layer moves at lower velocity compare to flow above it. The turbulent patches extended downstream and suppressed further propagation of the second shock because the diffracting shock has moved away from the wall curvature and is regaining its original shape before the start of diffraction process.

This shows that computation of various flow parameters in high speed flow such as drag, lift and pressure coefficient will be time dependent. The turbulent flow associated with the flow downstream of separation point requires further investigation to understand the flow physics around the region.

CONCLUSION

The flow induced by the diffracted shock wave on curved wall has been investigated and the following conclusions are deduced from the analysis:

1. The complex flow structure is a combination of many flow features that are time dependent

and they can only be clearly identified in large scale experiments

2. The flow features comprises of shear layer, oblique shock wave, second shock, main vortex and separating flow
3. The separation point moves upstream for incident shock Mach numbers, Mn = 1.5, remain stationary at Mach number 1.6 and moves downstream at higher Mach number
4. There are turbulent patches around the shear layer which propagates faster upstream than downstream.
5. There is need for further investigation of the behavior of the separation point between Mach Number 1.5 and 1.6 in an experimental facility of a higher scale than the present.

REFERENCES

Anderson, J. (2003). *Modern compressible flow with historical perspective.* New York: McGrawHill.

Berezkina, M. K. (2006). Diffraction of a two-shock configuration by a convex cylindrical surface. *Technical Physics 51*(7), 827-833.

Craig, R. S. (2005). Disturbances from shock/boundary layer interactions affecting upstream hypersonic flow. *35th AIAA Fluid Dynamics Conference and Exhibit.* Toronto, Ontario Canada.

Delery, J. (1985). Shock wave/Turbulent boundary layer interaction and its control. *Prog. Aerospace Science 22*, 209-280.

Law, C. (2005). Near-wall features in transient compressible flow on convex walls. In K. R. E.A. G Jagadeesh (Ed.), *25th Internationa lSymposium on Shock Waves.* Bangalore, India: Society for Shock Wave Research, IIS.

Law, C. , A. O. Muritala and B. W. Skews (2014). Unsteady separation behind a shock wave diffracting over curved walls *Shock Waves, Springer* 24(3), 283-294.

Menter, F. R. (1993). Zonal two equation k-*!* turbulence models for aerodynamic flows, AIAA 93-2906 ANSYSR® Fluent, Release 6.3, Help System, Theory

Guide, ANSYS, A. and O. Inc. Muritala (2011). *Separation of compressible flows over convex walls.* Ph. D. thesis, University of the Witwatersrand, South Africa, Faculty of Engineering and Built Environment.

Muritala, A. O. (2010). Near wall effects on the global flow behaviour behind a diffracted shock wave. In D. W. S. Kok (Ed.), *in Proceeding of Seventh South African Conference on Computational and Applied Mechanics* 543 – 548

Muritala, A. O., C. Law and B. W. Skews (2011). Shock wave diffraction on convex curved walls. *28th International Symposium on Shock Wave.* Manchester, United Kingdom.

Skews, B. W., C. Law, A. O. Muritala and S. Bode (2012). Shear layer behaviour resulting from shock wave diffraction. *Experiments in Fluids* 52(2), 417 - 424.

Skews, B. (1967). The shape of diffracting shock wavea. *Journal of Fluid Mechanics 29*, 297-304.

Skews, B. (1967b). The pertubed region behind a diffracting shock wave. *Journal of Fluid Mechanics* 29, 705-719.

Skews, B. (2005). Shock wave diffraction on multi-faceted and curved walls. *Shock waves 3*(14), 137 - 146.

Skews, B. M. (2010). Large scale shock wave diffraction experiments. *29th International Congress on High-Speed Photography*